

ISPC 23

Book of Extended Abstracts

**July 31th to August 4th, 2017
Montreal, Canada**

Antimicrobial NO_x generated by transient spark in atmospheric dry air and air with water electrospray

M. Janda¹, K. Hensel¹, B. Tarabová¹, V. Martišovič¹, Z. Machala¹.

¹*Division of Environmental Physics, Faculty of Mathematics, Physics and Informatics
Comenius University, Mlynská dolina F2, Bratislava 84248, Slovakia*

Abstract: Generation of nitrogen oxides (NO_x) was studied in a self-pulsing transient spark (TS) discharge in atmospheric pressure dry air and air with water electrospray. The precursors of NO_x production and the TS characteristics were studied by nanosecond time-resolved optical diagnostics. Thanks to the short (~10–100 ns) high current (~1 A) spark current pulses, highly reactive non-equilibrium plasma is generated. The NO_x production rate of $\sim 7 \times 10^{16}$ molecules/J was achieved in dry air, dependent on TS repetition frequency, i.e. power, which is related to the complex frequency-dependent NO₂/NO generating mechanisms. With water electrosprayed through the TS, gaseous NO_x formation was lowered but induced chemical changes in water make it of biomedical importance.

Keywords: non-thermal air plasma, nitrogen oxides, RONS, time-resolved optical diagnostic.

1. Introduction

In recent years, plasma science community largely focuses on novel biomedical applications of non-thermal (cold) atmospheric plasmas. Cold plasmas provide multiple agents that can efficiently kill bacteria and other hazardous microbes, and cause multiple biomedical and therapeutic effects in higher organisms. It is very important to assess the roles of the plasma agents involved in these processes. The major role in atmospheric pressure plasmas generated in air is typically attributed to reactive oxygen and nitrogen species (RONS) [1, 2].

When air plasmas interact with water, nitrites, nitrates, hydrogen peroxide and peroxyxynitrites are formed in this plasma activated water (PAW), which demonstrates strong antibacterial properties [2]. The aqueous RONS are formed from dissolved NO, NO₂, O₃, and OH radicals generated by plasma in the gas phase. Better understanding of the NO and NO₂ generation in the gas phase and its relation to the liquid phase are of great importance. This problem has already been partially addressed in exhaust gas cleaning applications by electrical discharges [3-5] who mostly studied NO reduction, or its oxidation to NO₂, and finally to HNO₃. A recent paper [6] investigated the NO and NO₂ formation related to their bactericidal effects in hybrid glow-spark discharges in air. Here we present a study focused on the synthesis of NO, NO₂ and their precursors (O and N radicals) by the transient spark (TS) discharge in dry air and air with electrosprayed water.

2. Experimental set-up

The experiments focused at optical diagnostics of TS were carried out in ambient air with the air flow velocity about 0.2 m.s⁻¹, perpendicular to the inter-electrode axis.

The distance d between the steel electrodes (point-to-point configuration with anode at the top) was varied between 4-7 mm. The radius of curvature of the sharp anode tip was of the order of 100 μm and that of the blunt cathode was of the order of a millimeter.

For the experiments focused at the NO_x production, the electrodes were placed in a closed tube with two valves for the gas inlet and outlet. These experiments were carried out in 1.3-2.6 l.min⁻¹ flow of synthetic air from the pressure tanks (N₂:O₂ = 4:1, N₂: 99.99% purity, O₂: 99.5% purity). We used a gas analyzer *Kane KM9106 Quintox* (to detect 0-1000 ppm NO and NO₂ with the 3 %accuracy) and Fourier-transform infrared (FTIR) spectrometer *Shimadzu IRAffinity-1S* (spectral resolution 0.5 cm⁻¹) to measure the gas composition after passing through the discharge reactor. In the experiments with water electrospray, deionized water was supplied by the syringe pump *New Era* through the high voltage needle electrode at flow rate 0.5 mL/min.

A dc HV power supply connected to the anode via a series resistor ($R = 9.84 \text{ M}\Omega$) was used to generate a positive TS discharge. The discharge voltage was measured by a HV probe *Tektronix P6015A* and the discharge current was measured on a 50 Ω or 1 Ω resistor shunt. Electric signals were recorded by a 200 MHz digitizing oscilloscope *Tektronix TDS2024*.

The time-resolved emission spectra were obtained using a 2-m monochromator *Carl Zeiss Jena PGS2* (spectral resolution 0.04-0.09 nm, depending on the entrance slit opening), covering the UV and VIS regions (200-800 nm), coupled with an intensified CCD camera *Andor Istar* (2 ns minimum gate).

The ICCD camera was triggered by a 5 V rectangular pulses generator with less than 5 ns rise time. This generator was triggered directly by the discharge current

signal, causing an additional delay of less than 10 ns. This delay, plus the delay caused by the transmission of the signal by BNC cables, was compensated by using a 10 m long optical cable (*Ocean Optics P400-10-UV-VIS*). During the measurements with the iCCD camera, an additional small resistor $r = 1 \text{ k}\Omega$ was attached directly to the anode. Its role was to eliminate the electric signals oscillations causing problems with the iCCD camera triggering (more details in [7]).

For fast measurements of the emission intensity evolution, we used a PMT module *Hamamatsu H955* (2.2 ns rise time). In order to isolate a specific spectral transition for PMT measurements, a bandpass interference filter (e.g. *Melles Griot 03 FIU127* for the N_2 (C-B, 0-0) transition), was inserted into the optical path. The PMT module signal was recorded using the oscilloscope. The experimental set-up is depicted in figure 1.

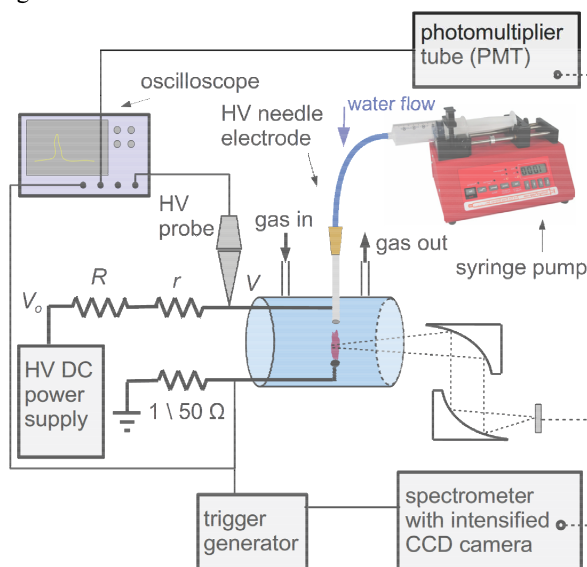


Figure 1. Simplified schematic of the experimental set-up.

3. Results and discussion

Transient spark is initiated by a streamer when the potential on the stressed electrode V reaches voltage V_{TS} , characteristic for the TS (figure 2). The streamer forms a relatively conductive plasma bridge between the electrodes leading to the transition to spark. During the spark phase, the electric circuit internal capacity discharges completely and the voltage on the HV electrode drops to almost zero (figure 2). The discharge current reaches a high value ($\sim 1\text{--}10 \text{ A}$). Transition to an arc after the spark phase is restricted by the large ballast resistor R . As a result, the plasma decays after the spark pulse. Eventually, the potential V on the anode gradually increases, as the capacitor C recharges. A new TS pulse, initiated by a new streamer, occurs when the potential V reaches the breakdown voltage V_{TS} again. The TS is thus based on repetitive charging and discharging of C with the characteristic repetition frequency f in the range 1–10 kHz.

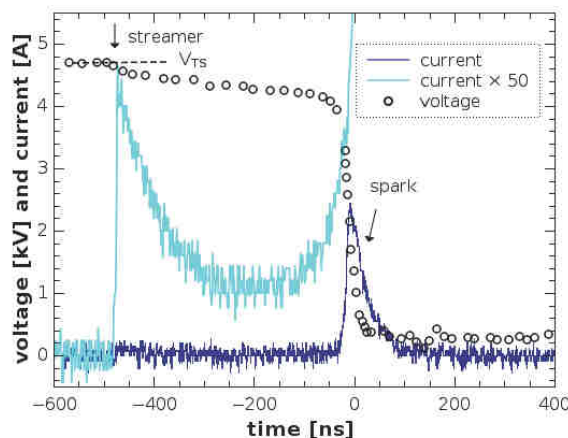


Figure 2. Typical TS voltage and current waveforms.

The time-integrated emission spectroscopy study confirmed that TS pulses generate highly reactive non-equilibrium plasma with excited atomic radicals (O^* , N^*), excited molecules N_2^* and ions N_2^{+*} . The TS characteristics change with increasing f , the spark pulses become smaller and broader. The emission characteristics reflect these changes. Below $\sim 3 \text{ kHz}$, the atomic line emission (O^* , N^*) and molecular N_2 2nd positive system dominates in the spectra, but at higher frequencies the atomic lines almost disappear. This might be interpreted as a decrease of the TS ability to produce radicals and to induce chemical changes at higher frequencies, but as we show in the following, it was not confirmed by the measurement of the nitrogen oxides densities.

Due to the increasing input power, the densities of both NO and NO_2 increase with f (figure 3). However, based on the NO and NO_2 generation rate in molecules per J energy delivered (figure 4), the NO generation efficiency tends to improve with increasing f , while the efficiency of the NO_2 generation decreases. The total NO_x , i.e. the sum of NO and NO_2 densities does not change significantly. These results show that the ability of TS to induce chemical changes cannot be evaluated using the total NO_x densities. The NO_x synthesis mechanism changes with the increasing TS repetition frequency.

Despite the fact that TS generates 'cold' non-equilibrium plasma, there is some gas preheating between the electrodes due to increasing f [8]. We therefore have to consider the Zeldovich thermal mechanism of the NO_x generation. This mechanism is initiated by the thermal decomposition of N_2 and O_2 into their atomic states at high temperature (above $\sim 1500 \text{ K}$). Next, both N and O atomic radicals are able to produce NO.

The temperature at which the initiating streamer starts (T_{str}) was only $\sim 600 \text{ K}$ at $f \approx 10 \text{ kHz}$ (figure 5). Temperature high enough to induce thermal decomposition of N_2 and O_2 is achieved only during the spark phase of the TS (T_{spark} , figure 5). However, the thermal decomposition of N_2 and O_2 could play an important role only if the temperature remained high enough for longer time after the spark.

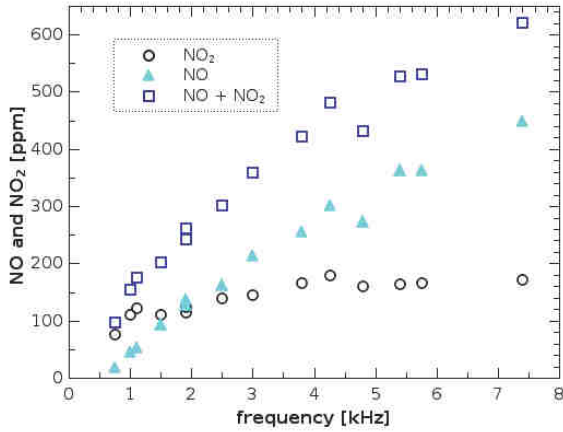


Figure 3. The NO and NO₂ densities produced by TS as functions of f .

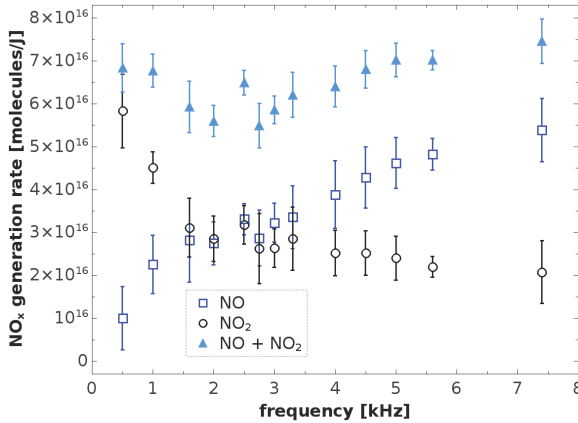


Figure 4. The NO and NO₂ generation rate [molecules/J] as a function of TS repetition frequency, $d \approx 6$ mm, $C \approx 35$ pF, $R = 9.24$ M Ω , $r = 0$ k Ω , averaged for flow rates 1.3-2.6 l.min⁻¹.

We approximated T_{str} and T_{spark} by the rotational temperature T_r of the N₂(C) species. The T_r was obtained by fitting the time-resolved (5-20 ns time window) experimental emission spectra of the N₂ 2nd positive system (0-0 transition) with the simulated ones, using Specair program [9]. However, this emission can be observed only for a short time after the streamer and spark current pulses (see figures 6 and 7, respectively), so we cannot measure the entire temperature evolution between two successive TS pulses. Thus, we cannot definitely assess the role of the thermal decomposition of N₂ and O₂, but we assume that other plasma processes are more important, since the electron density is very high during the spark phase of the TS [10].

Further details about these processes can be deduced from the emission profiles obtained by the PMT. The N₂(C) emission starts with the beginning of both streamer and spark current pulses. During the rising slope of the current pulses, the electrons must have enough energy to ionize N₂ and O₂. We therefore assume that the majority of the N₂(C) states are created by high energy electrons.

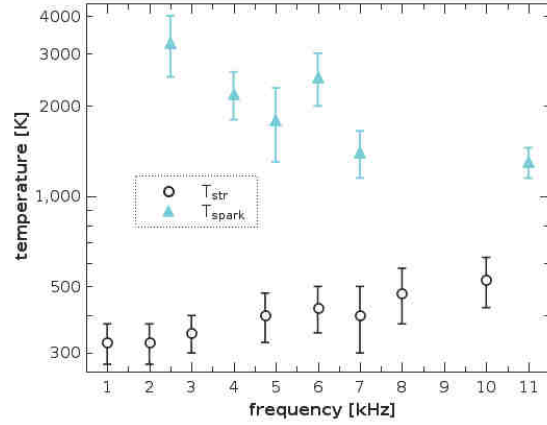


Figure 5. Temperature at the beginning of the streamer phase and the highest temperature during the spark phase of the TS as functions of f .

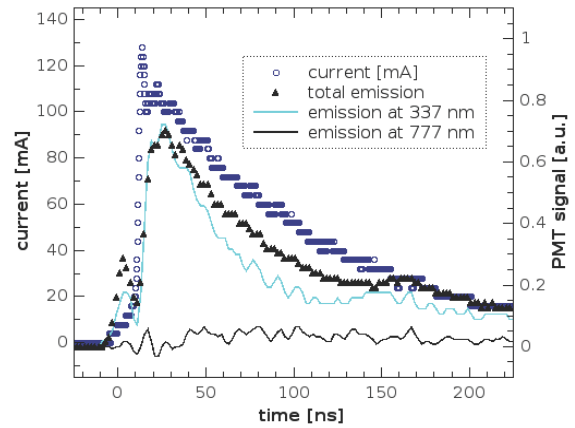


Figure 6. Typical PMT signals of the optical emission during the streamer phase of TS, $f \sim 2$ kHz.

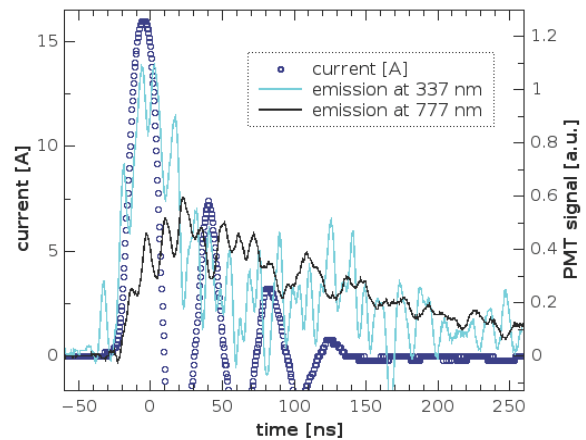


Figure 7. Typical PMT signals of the optical emission during the spark phase of TS, $f \sim 2$ kHz.

The quenching of excited N₂^{*} molecules, such as N₂(C) with molecular oxygen is probably one of the major sources of atomic oxygen. We should mention that

atomic O production need not be correlated with the O^* emission intensity. The emission from the excited O^* atoms can be observed almost exclusively during the spark phase, and its peak is slightly delayed with respect to the current rising edge (figure 7). The electron mean energy after the spark current pulse is around ~ 1 eV corresponding to the electron temperature ~ 10000 K [9]. We therefore suppose that O^* atoms are not produced by high energy electrons, but via stepwise processes thanks to the high density of relatively low energy electrons.

This can explain why there is almost no O^* emission during the streamer – the degree of ionization is much lower compared to spark. For the same reason, the atomic line emission intensity weakens at higher TS frequencies – spark current pulses are smaller and broader, and the electron density is lower [10]. It could also explain the increase of the NO/NO₂ ratio with increasing f . Thanks to the dissociative recombination, there might be enough O to produce not only NO, but also further oxidize it to NO₂.

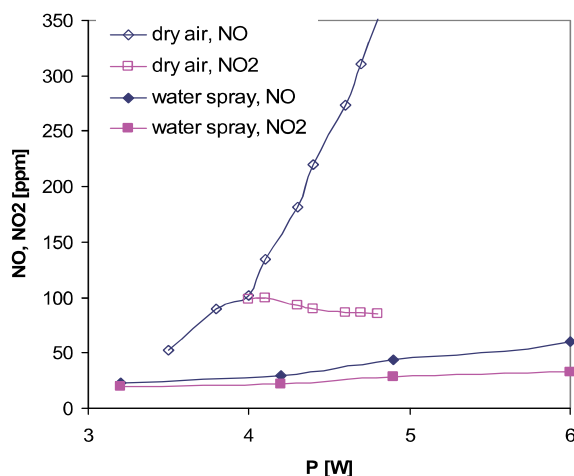


Figure 8. NO and NO₂ generation in TS in dry air vs. air with water electro-spray in dependence of discharge power.

Due to their easy dissolution in the water and possibly also due to the discharge cooling by water and thus lower NO_x formation, the NO_x densities generated by TS were found considerably lower in air humidified by the water electro-spray (Fig. 8). On the other hand, electro-sprayed water activated by TS discharge demonstrated strong antibacterial effects, especially due to the interacting nitrites (formed from gaseous NO_x), hydrogen peroxide (formed from H₂O molecules dissociating to OH radicals) and acidic milieu (due to formed nitric and nitrous acids) [2]. The effect of ozone potentially depleting NO in these lower temperature conditions has to be investigated in future.

4. Conclusions

We investigated the generation of NO and NO₂, significant biomedical and biocidal agents, by the self-pulsing Transient Spark (TS) discharge in atmospheric

pressure air. In dry synthetic air, the sum of NO and NO₂ densities more than 600 ppm was achieved with the power input below 6 W ($\sim 7 \times 10^{16}$ molecules/J) [11].

The TS characteristics change with the increasing TS repetition frequency. These changes also influence the generation of excited atomic species and nitrogen oxides. The atomic lines emission intensity decreases and the NO/NO₂ ratio increases with increasing TS repetition frequency. We attempted to explain these changes using temporal emission intensity profiles measured by photomultiplier tube.

The excited N₂^{*} molecules are produced by high energy electrons during the rising slope of the current pulses, both streamer and spark. These excited nitrogen molecules can lead to the sufficient atomic oxygen production necessary for the synthesis of NO. The excited atomic oxygen species are mostly produced during the spark current decreasing slope, probably via dissociative recombinations of O₂⁺. This provides additional atomic oxygen for the NO oxidation to NO₂. Since the TS spark pulses are getting broader and smaller with increasing frequency, this would explain why atomic lines weaken and NO/NO₂ ratio increases with the increasing TS frequency. Further research including kinetic modelling and measurement of O species in the ground state is required to prove this hypothesis.

In TS in air with electro-sprayed water, gaseous NO_x formation was lowered but chemical changes induced in water make it a strong antimicrobial agent.

5. Acknowledgement

Effort sponsored by the Slovak Research and Development Agency APVV-0134-12, and Slovak grant agency VEGA 1/0918/15.

6. References

- [1] D.B. Graves, *J. Phys. D: Appl. Phys.* **45** (2012) 263001.
- [2] Z. Machala, B. Tarabová, K. Hensel et al., *Plasma Process. Polym.* **10** (2013) 649-659.
- [3] B.M. Penetrante et al., *Appl. Phys. Lett.* **67** (1995) 3096.
- [4] M. Dors et al., *J. Electrostat.* **45** (1998) 25.
- [5] J.T. Herron, *Plasma Chem. Plasma Proc.* **21** (2001) 581.
- [6] M.J. Pavlovich, T. Ono, C. Galleher, B. Curtis, et al., *J. Phys. D: Appl. Phys.* **47** (2014) 505202.
- [7] M. Janda, V. Martišovič, Z. Machala, *Plasma Sources Sci. Technol.* **20** (2011) 035015.
- [8] M. Janda, Z. Machala, A. Niklová, V. Martišovič, *Plasma Sources Sci. Technol.* **21** (2012) 045006.
- [9] C.O. Laux, T.G. Spence, C.H. Kruger, R.N. Zare, *Plasma Sources Sci. Technol.* **12** (2003) 125.
- [10] M. Janda, V. Martišovič, K. Hensel, L. Dvonč, Z. Machala, *Plasma Sources Sci. Technol.* **23** (2014) 065016.
- [11] M. Janda, V. Martišovič, K. Hensel, Z. Machala, *Plasma Chem. Plasma Process.* **36**, 767 (2016)